Chemical Engineering Science 217 (2020) 115512

Contents lists available at ScienceDirect

Chemical Engineering Science

journal homepage: www.elsevier.com/locate/ces

Model reduction of aerobic bioprocess models for efficient simulation

Zhaoyang Duan [a], Terrance Wilms [b], Peter Neubauer [c], Costas Kravaris [a,*], Mariano Nicolas Cruz Bournazou [d]

[a] Artie McFerrin Department of Chemical Engineering, Texas A&M University, College Station, TX 77843, USA
[b] Chair of Measurement and Control, Department of Process Engineering, Technische Universität Berlin, D-10623 Berlin, Germany
[c] Department of Bioprocess Engineering, Institute of Biotechnology, Technische Universität Berlin, D-13355 Berlin, Germany
[d] DataHow AG, Zurich, Switzerland

HIGHLIGHTS

- In aerobic processes, the dynamics of the dissolved oxygen is usually very fast.
- Both continuous and fed-batch models can be reduced by approximating fast dynamics.
- The invariant manifold method leads to an accurate reduced model.
- The reduced model is useful for simplifying the observer design problem.

ARTICLE INFO

Article history:
Received 30 July 2019
Received in revised form 21 November 2019
Accepted 24 January 2020

Keywords:
Model reduction
Dissolved oxygen tension
Aerobic
Nonlinear dynamics
Observer

ABSTRACT

Owing to the increasing demand for large scale and high efficiency in manufacturing processes, computer aided tools for process operation and control are rapidly gaining popularity. An important state variable in aerobic processes is the dissolved oxygen, which can be easily measured online and is an important indicator of the metabolic activity. However, due to the fast kinetics of the oxygen transfer, dynamical models describing aerobic bioprocesses tend to be highly stiff. This can lead to significant numerical problems hampering its use for fixed step discretization methods and computationally costly applications such as computer fluid dynamics. In this work we use the slow-motion invariant manifold and the quasi steady state assumption methods to eliminate the differential equation describing the dissolved oxygen (the fast mode). By doing this, the tractability of the model is significantly increased with a neglectable loss in description power. The reduced model is also useful for simplifying the observer design problems, which is demonstrated by a state and parameter estimation example at the end of the work.

1. Introduction

A rapid shift in industry towards more sustainable manufacturing processes is desperately needed to meet the current environmental challenges. Biotechnology offers attractive alternatives to traditional chemical engineering processes for the production of pharmaceuticals (e.g. antibodies and insulin (Berlec and Štrukelj, 2013; Neubauer et al., 2013)), biodegradable materials, and renewable fuels (Gavrilescu and Chisti, 2005).

Nevertheless, bioprocesses typically lie behind chemical engineering solutions in terms of costs, developmental times, process efficiency, and reliability. For this reason, it is essential to tailor and apply existing process systems engineering (PSE) tools for process design, optimization and control (Rabitz et al., 1983; Wang et al., 2016; Westman and Franzén, 2015; Wang et al., 2014; Anane et al., 2017; Anane et al., 2019). But for this, an accurate and tractable mathematical description of the bioprocess is required. Once available, mathematical models can be used from regulatory agencies support as in Quality by Design (QbD) (Möller et al., 2019), over model-based process monitoring (e.g. soft sensors, nonlinear observers) and control (Dochain, 2013), up to plant optimization (Floudas and Gounaris, 2009; Koutinas et al., 2012), and to plant-wide optimization (Psaltis et al., 2013). And even though it is true that it is difficult to mathematically describe the dynamics of living organisms, macro-kinetic growth models offer a good trade-off between descriptive power and model tractability for bioprocesses (Mears et al., 2017; Enfors and Häggström, 2000; Cruz Bournazou et al., 2012).

The applicability of advanced model-based methods depends on the properties of the models used, such as accuracy, robustness, and identifiability. Stiffness, for example, increases the computa-

* Corresponding author.
E-mail addresses: zy.duan@tamu.edu (Z. Duan), terrance.wilms@tu-berlin.de (T. Wilms), peter.neubauer@tu-berlin.de (P. Neubauer), kravaris@tamu.edu (C. Kravaris), nicolas.cruz@tu-berlin.de (M.N. Cruz Bournazou).

https://doi.org/10.1016/j.ces.2020.115512
0009-2509/

tional burden and instability of the numerical integration. Differential equation systems that have both very fast and very slow modes will require very small discretization steps to catch all changes in the system and need long time spans to allow slow modes to come to equilibrium. Stiffness is especially inconvenient for fixed step discretization methods (e.g. full discretization) and large systems of partial differential equations (e.g. computational fluid dynamics). In aerobic bioprocesses, the big difference in dynamics between physicochemical phenomena and biological reaction can be very challenging. The dissolved oxygen, for instance, reveals important process insights, but is prone to cause stiffness due to its fast kinetics.

There are a number of methods that can be applied to reduce the order of chemical and biochemical models (Okino and Mavrovouniotis, 1998). Some of them are easy to implement and thereby widely used, such as the quasi-steady-state assumption (QSSA) method (Segel and Slemrod, 1989; Gorban, 2018) and singular perturbation method (Kokotovic et al., 1976; Kumar et al., 1998). However, due to the fact that these methods render some non-vanishing errors between the reduced model and the original one, the performance of the reduced model cannot be guaranteed for those applications that are sensitive to such errors. An alternative method to overcome this is the slow-motion invariant manifold method which can guarantee the convergence of the reduced model (Kazantzis et al., 2010). The invariant manifold method has been successfully applied to the fields of anaerobic digestion (Duan et al., 2017; Duan et al., 2017; Duan and Kravaris, 2018; Stamatelatou et al., 2009) and metabolic models (Roussel and Fraser, 2001), and is also widely used for the reduction of general chemical kinetics models (Gorban and Karlin, 2003; Gorban and Karlin, 2005; Chiavazzo et al., 2007). In this study, both the invariant manifold and the quasi-steady-state assumption methods are applied in search for a tractable but accurate description of aerobic bioprocesses. We demonstrate that it is possible to increase the tractability of aerobic bioprocess models with a minimal loss in accuracy.

We will first study the model reduction problem for aerobic processes. In Section 2, we analyze the dynamic properties of a basic 3-state aerobic system to demonstrate why model reduction is meaningful, and use the detailed *E. coli* model as a numerical example. In Section 3, both continuous and fed-batch process models will be reduced with the slow-motion invariant manifold method, in comparison to the simpler quasi-steady-state approximation approach. After the model reduction, in Section 4, we will work on an example to show how the reduced model could simplify the observer design problem to estimate the state and parameter.

2. Aerobic model and system properties

In aerobic processes, substrate is consumed by biomass in the presence of oxygen. Other organic and inorganic matters may also be involved in the process, such as acetate, enzyme, etc. For representative purposes, we will start with a basic aerobic model consisting of 4 states: biomass concentration (X) in [g/L], substrate concentration (S) in [g/L], dissolved oxygen tension (DOT) in [%] and the volume of culture medium (V) in [L]:

$$\begin{aligned}\frac{dS}{dt} &= -\frac{F}{V}(S - S_{in}) - q_s X\\ \frac{dX}{dt} &= -\frac{F}{V}X + \mu X\\ \frac{dDOT}{dt} &= K_L a(DOT^* - DOT) - Hq_o X\\ \frac{dV}{dt} &= F - F_{out}\end{aligned} \tag{1}$$

F and F_{out} are the inlet and outlet flow rates. The substrate is fed to the system with a concentration of S_{in}. In the DOT equation, $K_L a$ is the mass transfer coefficient for oxygen, DOT^* is the percentage of dissolved oxygen saturation and H is the Henry coefficient.

In real practice, the process is usually operated under substrate-limited conditions, where the oxygen is in excess. It is reasonable to assume that DOT is kept above the 20% level all the time and thereby the oxygen uptake rate q_o is independent of DOT. Then the biomass growth rate μ, the substrate and oxygen uptake rates q_s and q_o are functions of the substrate concentration only:

$$\begin{aligned}q_s &= q_{s\max}\frac{S}{S+K_S}\\ \mu &= Y_{x/s}q_s\\ q_o &= Y_{o/s}\cdot\left(q_s - \mu\cdot\frac{C_X}{C_S}\right)\end{aligned} \tag{2}$$

The definition for other coefficients are given in Table 1, as well as a set of representative parameter values to be used in the following sections, which is based on Enfors' book (Enfors and Häggström, 2000) and our experimental practices. As C_x and C_s in (2) can be treated as constant, q_o is then proportional to q_s. Thus, we can define an overall DOT to substrate yield coefficient $Y_o = Y_{o/s} - Y_{o/s}Y_{x/s}C_X/C_S$ and rewrite (2) as $q_o = Y_o q_s$.

There could be three operating conditions depending on the inlet and outlet flows: batch, fed-batch and continuous operations. The batch reactor has neither inflow nor outflow: $F = F_{out} = 0$. The fed-batch reactor has only inflow but no outflow: $F_{out} = 0$. In continuous operation, the rate of the inlet flow equals to that of the outflow: $F = F_{out} \neq 0$. Therefore, the volume of culture remains constant in both batch and continuous reactors, and the state V in model (1) can be dismissed for these operations. Particularly, the continuous reactor model can be written as:

$$\begin{aligned}\frac{dS}{dt} &= -D(S - S_{in}) - q_s X\\ \frac{dX}{dt} &= -DX + \mu X\\ \frac{dDOT}{dt} &= K_L a(DOT^* - DOT) - Hq_o X\end{aligned} \tag{3}$$

where $D = F/V$ represents the dilution rate and is defined as the ratio of inlet flow rate over the culture medium volume.

To study the properties of aerobic systems, the continuous process would be a good starting point. For the model (3), there are two steady states: one is a trivial steady state, where the biomass is washed out; and the other non-trivial steady state can be calculated as:

$$\begin{aligned}S_s &= \frac{-DK_s}{-Y_{x/s}q_{s\max} + D}\\ X_s &= Y_{x/s}(S_{in} - S_s)\\ DOT_s &= DOT^* - \frac{Y_o HD(S_{in} - S_s)}{K_L a}\end{aligned}$$

Table 1
Parameter values.

S_{in}	Organic substrate concentration in feed	20	g/L
$q_{s\max}$	Maximum aerobic substrate uptake rate	1.5	g/gh
K_s	Half-saturation constant for organic substrates	0.05	g/L
DOT^*	Percentage of dissolved oxygen saturation	100	%
$K_L a$	Mass transfer coefficient for oxygen	800	h^{-1}
$Y_{x/s}$	Specific aerobic yield for substrate	0.56	g/g
$Y_{o/s}$	Specific yield of DOT to substrate	1.217	%/g
H	Henry coefficient	14000	
D	Dilution rate	0.4	h^{-1}
C_s	Carbon content of substrate	0.487	gC/gX
C_x	Carbon content of biomass	0.391	gC/gX

By linearizing model (3) around this steady state, we get the following expression:

$$\begin{bmatrix} \dot{S} \\ \dot{X} \\ \dot{DOT} \end{bmatrix} = \begin{bmatrix} -D - X_s \frac{dq_s}{dS}\Big|_{s.s.} & -\frac{D}{Y_{x/s}} & 0 \\ -Y_{x/s} X_s \frac{dq_s}{dS}\Big|_{s.s.} & 0 & 0 \\ -HY_o X_s \frac{dq_s}{dS}\Big|_{s.s} & -\frac{Y_o}{Y_{x/s}} DH & -K_L a \end{bmatrix} \begin{bmatrix} S - S_s \\ X - X_s \\ DOT - DOT_s \end{bmatrix} \tag{4}$$

and the corresponding eigenvalues:

$$\lambda_1 = -D$$
$$\lambda_2 = -K_L a$$
$$\lambda_3 = -\frac{q_{s\max} K_s X_s}{(S_s + K_s)^2} = \frac{Y_{x/s} q_{smax} - D}{Y_{x/s} q_{smax} K_s} (S_{in} Y_{x/s} q_{smax} - S_{in} D - D K_s)$$

Apparently, all three eigenvalues are negative and this is a stable steady state. It can be seen that the eigenvalue λ_1 equals to the negative dilution rate. The value of λ_2 is the mass transfer coefficient for oxygen $-K_L a$, which is usually a very large number such that $K_L a \gg D$ and λ_3 is also small compared to $K_L a$. Since these eigenvalues are of different orders of magnitude, the process is comprised of fast and slow dynamics, with $\lambda_2 = -K_L a$ to be the fast eigenvalue, $\lambda_1 = -D$ and λ_3 related to reaction dynamics to be the slow. This spectral gap is more explicit given the numbers of eigenvalues calculated with the parameters in Table 1: $\lambda_1 = -0.4, \lambda_2 = -800$ and $\lambda_3 = -91.98$.

Note that the linearized matrix in (4) is a lower block triangular matrix, with $-K_L a$ being the right bottom block, which is the value of the fast eigenvalue λ_2. The left upper block governs the dynamics of the first two states S and X, with only slow eigenvalues, and therefore they are the slow states. And the state DOT is the fast state that associates with the fast eigenvalue $\lambda_2 = -K_L a$. Consequently, the entire process has serial structure, with the slow dynamics followed by the fast dynamics.

The physiology of *E. coli*, which has been described mathematically and applied in various studies (Anane et al., 2017; Haby et al., 2018; Neubauer et al., 2013), can be used as an example to demonstrate these dynamic properties in a specific application. An *E. coli* model can be written as:

$$\begin{aligned} \frac{dS}{dt} &= -\frac{F}{V}(S - S_{in}) - q_s X \\ \frac{dX}{dt} &= -\frac{F}{V} X + \mu X \\ \frac{dA}{dt} &= -\frac{F}{V} A + q_A X \\ \frac{dDOT}{dt} &= K_L a (DOT^* - DOT) - q_o X H \\ \frac{dV}{dt} &= F - F_{out} \end{aligned} \tag{5}$$

This dynamic model is comprised of five ODEs describing five state variables, namely biomass X, extracellular concentrations of substrate (glucose) S, acetate A, dissolved oxygen DOT, and culture volume V. They are modelled in a standard form, which can be easily transformed to a continuous, fed-batch or batch process model.

The auxiliary algebraic equations, coupled with the ODEs to form the kinetic model, are listed as follows; they describe the biomass formation, and the intracellular interactions relating substrate, oxygen and acetate consumption:

$$\begin{aligned} q_s &= \frac{q_{smax}}{1 + \frac{A}{K_{ia}}} \cdot \frac{S}{S + K_s} \\ q_{sof} &= \frac{P_{Amax} q_s}{q_s + K_{ap}} \\ q_{sox} &= (q_s - q_{sof}) \\ p_A &= q_{sof} Y_{as} \\ q_{sA} &= \frac{q_{Amax}}{1 + \frac{q_s}{K_{is}}} \frac{A}{A + K_{sa}} \\ q_A &= p_A - q_{sA} \\ q_o &= (q_{sox} - q_m) Y_{os} + q_{sA} Y_{oa} \\ \mu &= (q_{sox} - q_m) Y_{em} + q_{sof} Y_{xsof} + q_{sA} Y_{xa} \end{aligned}$$

Note that under the assumption that $DOT > 20\%$, the kinetics functions are still independent of DOT. An elaborate description of this model and parameter values can be found in the publication of Anane et al. (2017).

For a continuous process with $D = 0.15\ \mathrm{h}^{-1}$, $S_{in} = 20$ g/L and $K_L a = 800\ \mathrm{h}^{-1}$, the non-trivial steady state can be calculated numerically as:

$$S_s = 0.0273 \quad X_s = 11.37 \quad A_s = 0.0296 \quad DOT_s = 38.67.$$

After linearization around the steady state, the state linear matrix is

$$\begin{bmatrix} -63.37 & -0.2634 & 2.36 & 0 \\ 28.89 & 0 & 3.728 & 0 \\ 13.02 & 0.0004 & -9.042 & 0 \\ -1100000 & -4315 & -22955 & -800 \end{bmatrix} \tag{6}$$

and the eigenvalues around the steady state are calculated as

$$\lambda_1 = -800 \quad \lambda_2 = -63.81 \quad \lambda_3 = -8.445 \quad \lambda_4 = -0.1512.$$

It is evident that the system (5), even with more detailed kinetics, is comprised of both fast (λ_1) and slow (λ_2, λ_3 and λ_4) eigenvalues. Similarly to the previous basic system (3), the linear state matrix is also block lower triangular. Therefore, it can be concluded that DOT is the fast state that corresponds to the fast eigenvalue ($-K_L a$) in the *E. coli* model.

Based on this fact, it's meaningful to properly eliminate the very fast dynamics associated with the state DOT in dynamic model (3), so that the stiffness issue can be avoided when applying this model to biology and bioengineering applications.

For fed-batch operations, the system is different as there is no steady state and it is meaningless to study their eigenvalues. However, inspired by the idea from continuous processes, we will still apply similar approaches to probe the fed-batch models, and then show that the reduced model is also valid for the fed-batch case as long as $K_L a$ is large.

3. Model reduction

It has been shown in Section 2 that the continuous aerobic process is comprised of fast and slow modes. Therefore, the models are eligible for further simplification by assuming the fast dynamics to be instantaneous and approximate the fast state as a function of other slow states. One approach for implementation is to find the slow-motion invariant manifold of the system and use it to approximate the fast state. A detailed tutorial and explanation about this method can be found in some previous work (Kazantzis et al., 2010; Duan et al., 2017; Stamatelatou et al., 2009).

Another widely used, simple but less accurate approach is the QSSA method. It assumes that the fast state reaches its steady state instantaneously, and thus approximating the differential equation of that state to be zero. One can directly solve the algebraic equa-

tions by setting the differential equations of the fast states to be zero.

In the following part, we will apply both methods to reduce the order of continuous and fed-batch models, and compare the results.

3.1. Continuous processes

Consider a dynamic system of the form:

$$\frac{dx_s}{dt} = F_s(x_s)$$
$$\frac{dx_f}{dt} = F_f(x_s, x_f)$$

with x_s and x_f being the vectors of slow and fast states, where the slow dynamics F_s are followed by the fast dynamics F_f. The fast states can then be approximated by the slow-motion invariant manifold $x_f = T(x_s)$ where $T(x_s)$ satisfies the following invariance equation (Kazantzis et al., 2010)

$$\frac{\partial T(x_s)}{\partial x_s} F_s(x_s, T(x_s)) = F_f(x_s, T(x_s))$$

In the basic continuous aerobic digestion model (1), the slow-motion invariant manifold $T(S,X)$ can be used to approximate the fast state *DOT*, and it should satisfy

$$\begin{aligned}&\frac{\partial T(S,X)}{\partial X}(-DX + \mu(S)X) + \frac{\partial T(S,X)}{\partial S}[D(S_{in} - S) - q_s(S)X] \\ &= K_L a(DOT^* - T(S,X)) - Hq_o(S)X\end{aligned} \tag{7}$$

This is a first order nonlinear partial differential equation, whose exact solution is difficult to find in closed form. But an asymptotic solution can be derived by using perturbation analysis. As $K_L a$ is a large number, it is evident that $\epsilon = 1/K_L a$ is a very small parameter that can be used for perturbation analysis. Dividing both sides of Eq. (7) by $K_L a$, and we have

$$\begin{aligned}&\varepsilon\frac{\partial T(S,X)}{\partial X}(-DX + \mu(S)X) + \varepsilon\frac{\partial T(S,X)}{\partial S}[D(S_{in} - S) - q_s(S)X] \\ &= DOT^* - T(S,X) - \varepsilon Hq_o(S)X\end{aligned}$$

or equivalently,

$$\begin{aligned}&\varepsilon\frac{\partial T(S,X)}{\partial X}\left(-DX + Y_{x/s}q_{s\max}X\frac{S}{S+K_S}\right) \\ &+ \varepsilon\frac{\partial T(S,X)}{\partial S}\left[D(S_{in} - S) - q_{s\max}X\frac{S}{S+K_S}\right] = DOT^* - T(S,X) \\ &- \varepsilon Y_o q_{s\max}HX\frac{S}{S+K_S}.\end{aligned} \tag{8}$$

Expanding $T(S,X)$ in asymptotic series in terms of the small parameter ϵ:

$$T(S,X) = P_0(S,X) + P_1(S,X)\cdot\varepsilon + P_2(S,X)\cdot\varepsilon^2 + P_3(S,X)\cdot\varepsilon^3 \ldots \tag{9}$$

and substituting (9) into (8), we get

$$\begin{aligned}&\left(\frac{\partial P_0}{\partial X}\varepsilon + \frac{\partial P_1}{\partial X}\varepsilon^2 + \frac{\partial P_2}{\partial X}\varepsilon^3\right)\left[\left(-DX + Y_{x/s}q_{s\max}X\frac{S}{S+K_S}\right)\right] \\ &+ \left(\frac{\partial P_0}{\partial S}\varepsilon + \frac{\partial P_1}{\partial S}\varepsilon^2 + \frac{\partial P_2}{\partial S}\varepsilon^3\right)\left[D(S_{in} - S) - q_{s\max}X\frac{S}{S+K_S}\right] \\ &= -\left(P_0 + P_1\varepsilon + P_2\varepsilon^2 + P_3\varepsilon^3\right) + \left(DOT^* - \varepsilon Y_o q_{s\max}HX\frac{S}{S+K_S}\right).\end{aligned} \tag{10}$$

We can solve for the unknown terms P_i in (10) by matching the coefficients of the terms in ϵ from lower order to higher order. The result with up to the second order in ϵ is:

$$\begin{aligned}P_0 &= DOT^* \\ P_1 &= -Y_o HXq_s(S) \\ P_2 &= q_o H(-DX + \mu(S)X) + Y_o XH\tfrac{dq_s}{dS}[-D(S - S_{in}) + q_s(S)X]\end{aligned}$$

where

$$\frac{dq_s}{dS} = q_{smax}\frac{K_S}{(S+K_S)^2}$$

The slow motion invariant manifold for *DOT* can be expressed as

$$\begin{aligned}T(S,X) &= P_0(X,S) + P_1(X,S)\cdot\tfrac{1}{K_L a} + P_2(X,S)\cdot\tfrac{1}{K_L a^2} + O\left[\left(\tfrac{1}{K_L a}\right)^3\right] \\ &= DOT^* - \tfrac{XHY_o q_{s\max}}{K_L a}\tfrac{S}{S+K_s} \\ &\quad + \tfrac{1}{K_L a^2}\left\{q_o H(-DX + \mu(S)X) + Y_o XH\tfrac{dq_s}{dS}[-D(S - S_{in}) + q_s(S)X]\right\} \\ &\quad + O\left[\left(\tfrac{1}{K_L a}\right)^3\right]\end{aligned} \tag{11}$$

Therefore, the reduced model becomes

$$\begin{aligned}\frac{dS}{dt} &= -D(S - S_{in}) - q_s(S)X \\ \frac{dX}{dt} &= -DX + \mu(S)X \\ DOT &= T(S,X)\end{aligned} \tag{12}$$

where

$$\mu(S) = Y_{x/s}q_s$$
$$q_s(S) = q_{s\max}\tfrac{S}{S+K_S}$$

Fig. 1 illustrates the approximation of the dynamics (3) through the reduced model (12) arising from the invariant manifold method. For an initial condition $S(0) = 0.008$ g/L, $X(0) = 1.6$ g/L, $DOT(0) = 25$ %, the blue line represents the dynamic response of the exact model (3), whereas the red dotted line of the reduced model (12) initialized at the same $S(0)$ and $X(0)$, but with $DOT(0) = T(S(0), X(0))$. The exact trajectory of the system involves an initial phase where the system approaches the invariant manifold very fast, and second phase where the system slowly moves along the invariant manifold and eventually reaches the steady state. The model reduction approximation involves projecting the initial state on the slow-motion invariant manifold, by essentially ignoring the very fast transient of approach to the invariant manifold. With the reduced system directly starting on the invariant manifold, all its trajectories will lie on it, as a consequence of the defining property of the invariant manifold (Kazantzis et al., 2010). So, the reduced model's state will involve an initial error that will rapidly decay at early stage and exponentially converge to zero.

Alternatively, one can use the QSSA method to find an approximation by assuming the state *DOT* to be at steady state:

$$\frac{dDOT}{dt} = K_L a(DOT^* - DOT) - q_o(S)XH \approx 0$$

The result from quasi-steady-state approximation is

$$DOT \approx DOT^* - \frac{XHY_o q_{s\max}}{K_L a}\frac{S}{S+K_s}$$

Comparing the results from slow motion invariant manifold method and the QSSA, it can be seen that they are consistent with each other since the result from QSSA method matches the first two terms of the slow invariant manifold in (11). As the QSSA result has an error of $O(1/K_L a^2)$, when $K_L a$ is a very large number,

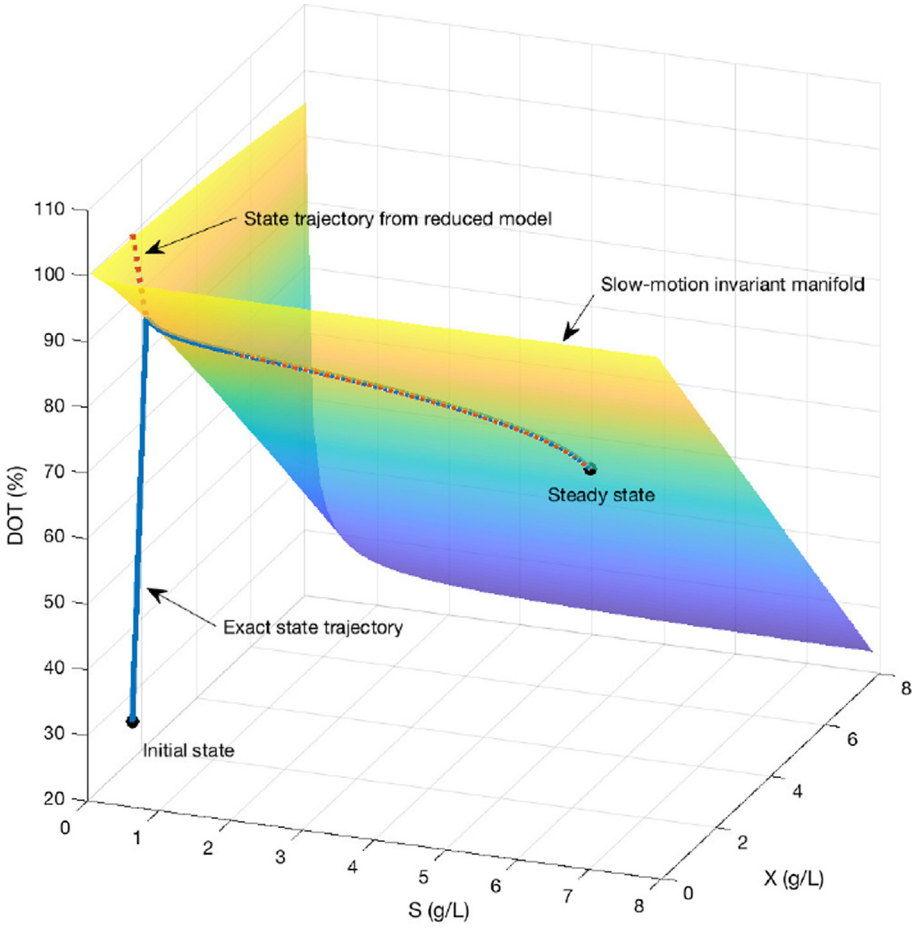

Fig. 1. The evolution of real and reduced states on the invariant manifold.

this approximation is expected to show a good match to the real fast state. At the same time, it should also be noted that the higher order terms in the series solution for slow-motion invariant manifold could provide additional corrections to the leading terms, to render a more accurate approximation. One can decide how many terms to keep in the series solution, depending on the need for accuracy and calculation cost.

For the continuous operation of *E. coli* model (5), a similar model reduction approach can be performed. The asymptotic series expansion of the slow-motion invariant manifold up to the second order term can be calculated as:

$$T(S,X,A) = DOT^* + \frac{1}{K_L a}(-XHq_o) + \frac{1}{K_L a^2}\{q_o H(-DX+\mu X) + XH\frac{\partial q_o}{\partial S}[D(S_{in}-S)-q_s X] + XH\frac{\partial q_o}{\partial A}(-DA+q_a X)\} + O\left[\left(\frac{1}{K_L a}\right)^3\right] \quad (13)$$

The QSSA result is again the same with the first two terms in series expansion for the slow-motion invariant manifold.

To verify the accuracy of the reduced model, we simulate the basic aerobic process in Fig. 2 and the *E. coli* process in Fig. 3. At time 2 h and 4 h for the basic aerobic process, and at time 10 h and 20 h for the *E. coli* process, $K_L a$ is changed from 800 to 1000 and 900, as a result of some step change in oxygen flow rate and/or stirrer speed, to perturb the system. It can be observed from the graphs in both figures that the reduced models are in good agreement with the detailed ones most time except for the very fast changing period with peaking mismatch. The second graph, which depicts the error, clearly indicates these peaks, for whenever $K_L a$ value changes. The peaking issues at changing points are due to the elimination of the fast modes in reduced models, and thereby the reduced models are not capable of capturing the very fast dynamics when system undergoes a sudden change. In the third graph, which is a zoom-in view for the errors, the small size of error of orange lines indicates that even the result from QSSA method (corresponding to the first two terms in Eq. (11)) is with satisfactory accuracy, but the presence of second order term (red lines) makes the reduced model even more precise. But whenever $K_L a$ value changes, there are noticeable peaking errors for both reduced models.

As a conclusion, for the typical aerobic systems, while the slow invariant manifold method guarantees the good accuracy and convergence of the reduced model, the result from QSSA method is also fairly accurate as long as $K_L a$ is very large. However, the result from QSSA method may not always be accurate enough for systems with moderately large $K_L a$. For example, with $K_L a = 30\ \mathrm{h}^{-1}$, $Y_o = 0.107$ and $S_{in} = 10$ g/L, running a new simulation leads to the results in Fig. 4. While the invariant manifold with up to the second order term still show good accuracy, one can notice the significant error between the QSSA approximation with the exact one, especially in the transient phase.

The reduced model for batch processes can be treated as a simplified version of the continuous process with $D = 0\ \mathrm{h}^{-1}$.

3.2. Fed-batch

It has been demonstrated that the slow-motion invariant manifold could be used to approximate the fast state locally around the

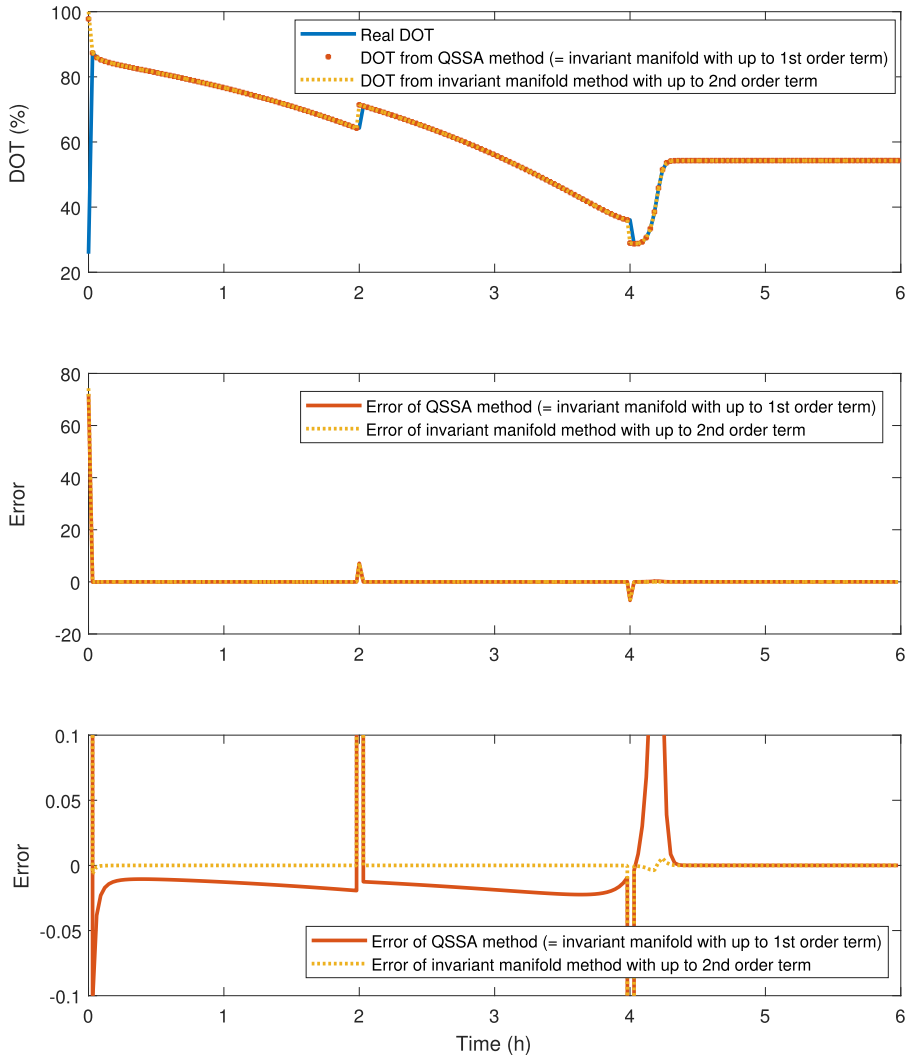

Fig. 2. Simulation of the basic continuous aerobic process.

steady state. For the fed-batch operation, a local analysis is no longer meaningful. Therefore, in order to apply a similar method, we need to also show that the calculated slow-motion invariant manifold would asymptotically approach the real state under fed-batch operations over the entire feasible domain. By setting $F_{out} = 0$ in (1), the fed-batch process can be described as follows:

$$\begin{aligned} \frac{dS}{dt} &= -\frac{F}{V}(S - S_{in}) - q_s X \\ \frac{dX}{dt} &= -\frac{F}{V}X + \mu X \\ \frac{dDOT}{dt} &= K_L a(DOT^* - DOT) - Hq_o X \\ \frac{dV}{dt} &= F \end{aligned} \tag{14}$$

To calculate the slow invariant manifold, we follow the same procedure as for the continuous process. The corresponding slow-motion invariant manifold equation for system (14) is:

$$\begin{aligned} &\frac{\partial T(S,X)}{\partial X}\left(-\frac{F}{V}X + \mu(S)X\right) + \frac{\partial T(S,X)}{\partial S}\left\{\frac{F}{V}(S_{in} - S) - q_s(S)X\right\} \\ &+ \frac{\partial T(S,X)}{\partial V}F \\ &= K_L a(DOT^* - T(S,X)) - q_o(S)HX \end{aligned} \tag{15}$$

Similarly, we define $\epsilon = 1/K_L a$ as the small parameter. Dividing both sides of the equation by $K_L a$, we have

$$\begin{aligned} &\varepsilon\frac{\partial T(S,X)}{\partial X}\left(-\frac{F}{V}X + \mu(S)X\right) + \varepsilon\frac{\partial T(S,X)}{\partial S}\left[\frac{F}{V}(S_{in} - S) - q_s(S)X\right] \\ &+ \varepsilon\frac{\partial T(S,X)}{\partial V}F \\ &= DOT^* - T(S,X) - \varepsilon q_o(S)HX \end{aligned} \tag{16}$$

Expanding $T(S,X)$ in asymptotic series in terms of the small parameter, substituting the expansion for $T(S,X)$ into the Eq. (16), and solving the equation, we will get the slow invariant manifold as:

$$\begin{aligned} DOT(X,S,V) &= P_0(X,S,V) + \tfrac{P_1(X,S,V)}{K_L a} + \tfrac{P_2(X,S,V)}{K_L a^2}\ldots \\ &= DOT^* - \tfrac{XHY_o q_{s\max}}{K_L a}\tfrac{S}{S+K_s} \\ &\quad + \tfrac{1}{K_L a^2}\left\{q_o H\left(-\tfrac{F}{V}X + \mu(S)X\right)\right. \\ &\quad \left. + Y_o XH\tfrac{dq_s}{dS}\left[\tfrac{F}{V}(-S - S_{in}) + q_s(S)X\right]\right\} + O\left[\left(\tfrac{1}{K_L a}\right)^2\right] \end{aligned} \tag{17}$$

Note that this result is very similar to that of the continuous model, except for the substitution of D with F/V. However, one may notice a significant difference between them when higher order terms are calculated.

Next we will show that this calculated slow invariant manifold will asymptotically approach the real state.

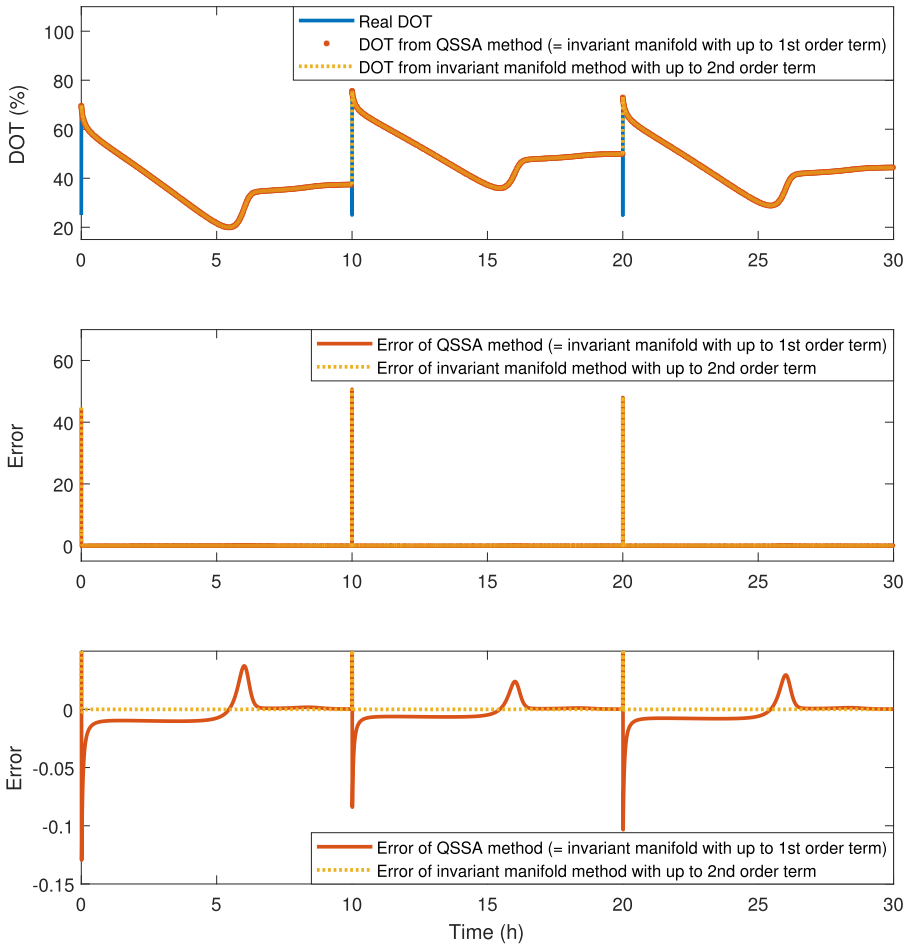

Fig. 3. Simulation of the *E. coli* continuous process.

Proposition. Let $DOT\prime(S(t),X(t),V(t))$ be the unique solution of the invariance Eq. (15) for the model (1), and $(S(t),X(t),DOT(t),V(t))$ a solution curve of model (1). The dynamics of the off-manifold coordinate $z = DOT(t) - DOT\prime(S(t),X(t),V(t))$ decays exponentially and the rate of decay is governed by K_La.

Proof. Since $DOT\prime$ is the solution of Eq. (15), it holds that:

$$\frac{\partial DOT\prime(S,X,V)}{\partial S} f_1(S,X,V) + \frac{\partial DOT\prime(S,X,V)}{\partial X} f_2(S,X,V) + \frac{\partial DOT\prime(S,X,V)}{\partial V} F = -K_La \cdot DOT\prime + K_La \cdot DOT^* - Y_o q_{s\max} XH \frac{S}{S+K_S}$$

The dynamics of $z = DOT - DOT\prime$ is described by the following nonlinear differential equation

$$\begin{aligned}\frac{dz}{dt} &= \frac{dDOT}{dt} - \frac{dDOT\prime}{dt} \\ &= \left(-K_La \cdot DOT - Y_o q_{s\max} \tfrac{S}{S+K_S} XH + K_La \cdot DOT^*\right) \\ &\quad - \left(\frac{\partial DOT\prime(S,X,V)}{\partial S} f_1(S,X,V) + \frac{\partial DOT\prime(S,X,V)}{\partial X} f_2(S,X,V) + \frac{\partial DOT\prime(S,X,V)}{\partial V} F\right) \\ &= \left(-K_La \cdot DOT - Y_o q_{s\max} XH \frac{S}{S+K_S}\right) - \left(-K_La \cdot DOT\prime - Y_o q_{s\max} XH \tfrac{S}{S+K_S}\right) \\ &= -K_La \cdot z\end{aligned}$$

So the off-manifold coordinate will exponentially decay to 0 with the rate of K_La.

The result calculated from quasi-steady-state approximation remains the same as the one for continuous model. That's because the first two terms contain no dilution-related terms.

For the *E. coli* model (5), the fed-batch result also turns out to be similar with the continuous one. The reader can refer to the reduced continuous *E. coli* model (13) and substitute the dilution rate D with F/V for up to the second order terms to find the reduced fed-batch model.

In Fig. 5, the same simulation as in Fig. 2 is done for the basic aerobic process model under fed-batch operation. It can be noted that both the reduced models derived using slow-motion invariant manifold and from QSSA method have similar performance as the continuous model. We skip the simulation result for fed-batch *E. coli* model as it shows similar behaviour as the continuous case.

4. Application of reduced model: simplified observer design for aerobic process monitoring

The lack for affordable and reliable sensors that can measure all states on-line poses challenges to the bioreactor operation. It also makes advanced monitoring and control for these processes a tough problem. For this reason, an observer, also known as a soft sensor, becomes useful as it could estimate some inaccessible state information and unknown parameter values based on the measured variables with certain algorithms. Common observer techniques include the Luenberger observer (Luenberger, 1964) and the Kalman filter (Kalman, 1960; Welch et al., 1995). There are a number of published books and articles that give introduction on the theory and their applications on bioreactors (Dochain, 2003; Kazantzis and Kravaris, 1998; Krämer and King., 2019; Kravaris et al., 2004, 2013). In this part, we will use the Luenberger observer as an example.

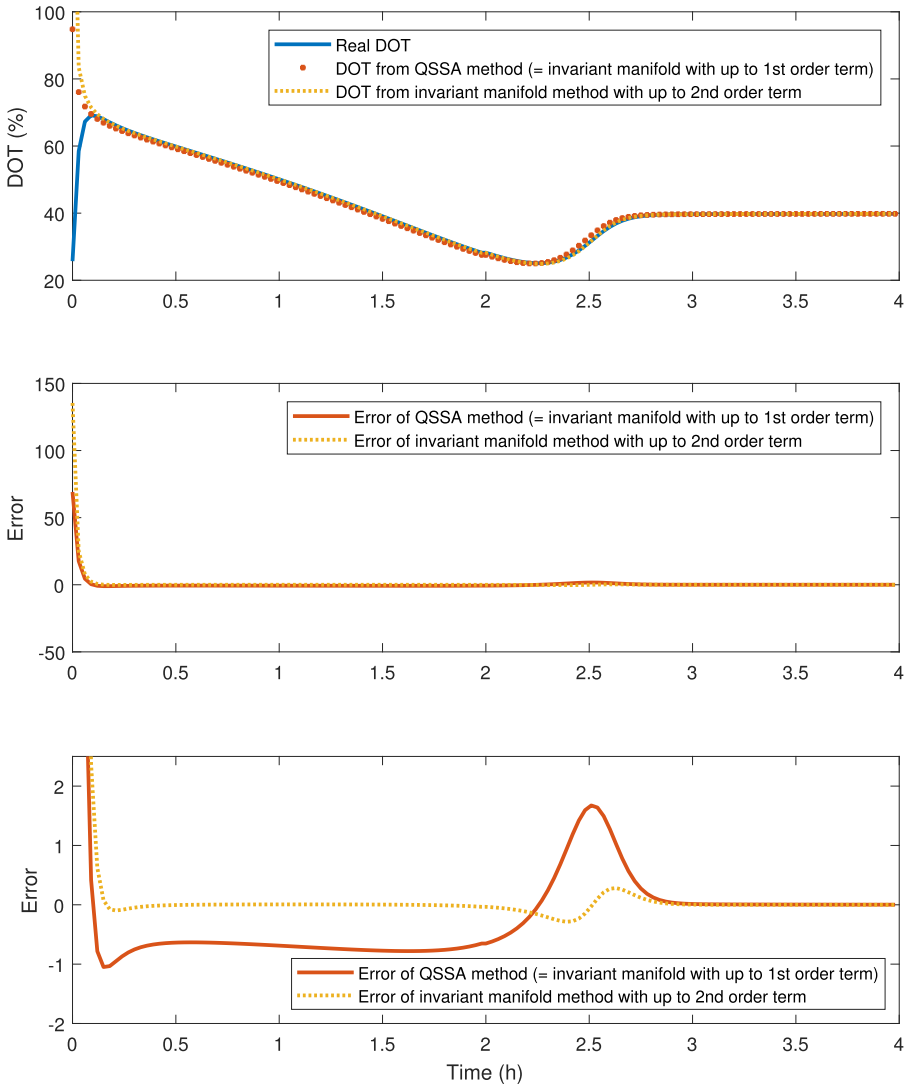

Fig. 4. Simulation of an arbitrary continuous process with small K_La.

To estimate the unmeasured state variables for an observable system, the traditional full-order identity observer would introduce a new estimator state for each state with proper dynamics, and these new estimated states would asymptotically approach the real states with the information from measurements. This requires the engineer to have relevant background knowledge in order to perform observer design. And the presence of high order observers will increase the computational effort as well. Now, with the availability of the reduced model, state estimation becomes easier, because some of the unknown states could be directly calculated from the algebraic equations instead of tackling the original differential equation system. We will demonstrate an example for the fed-batch system.

For the basic 4-state fed-batch aerobic process, the dissolved oxygen tension *DOT* and the volume of culture are usually measured continuously on-line, but the biomass and the substrate concentration X and S are either hard to measure or can only be measured offline with a relatively slow sampling rate due to the sensor limitation. And the value of inlet flow rate F might be hard to be accurately measured in some applications. In this case, we assume the measurements to be available for *DOT* and X, and the estimation for state variable S is needed. Also, the inlet flow rate F is piecewise time variant and unknown.

At first, we consider all the measurements to be continuous. The traditional observer is a full-order constant-gain Luenberger observer with a parameter estimator as follow:

$$\frac{d}{dt}\begin{bmatrix}\hat{S}\\ \hat{X}\\ D\hat{O}T\\ \hat{V}\\ \hat{F}\end{bmatrix}=\begin{bmatrix}-\frac{\hat{F}}{\hat{V}}\left(\hat{S}-S_{in}\right)-\hat{X}q_s\left(\hat{S},D\hat{O}T\right)\\ -\frac{\hat{F}}{\hat{V}}\hat{X}+Y_{x/s}\hat{X}q_s\left(\hat{S},D\hat{O}T\right)\\ K_La\left(DOT^*-D\hat{O}T\right)-HY_o\hat{X}q_s\left(\hat{S},D\hat{O}T\right)\\ \hat{F}\\ 0\end{bmatrix}+L\begin{bmatrix}X-\hat{X}\\ DOT-D\hat{O}T\\ V-\hat{V}\end{bmatrix}$$

where L is designed using classical pole placement methods.

For the reduced model, with the measurement of X, *DOT* and V, unknown inlet flow rate F can be obtained by calculating the time derivative of V, and S can be solved directly from the algebraic Eq. (17) by substituting X, *DOT* and V with the measured data at every sampling point. To simulate this process, we use the parameter values in Table 1, with the initial culture volume $V = 0.2$ L, and the initial $F = 0.1$ L/h. F is stepped up to 0.12, 0.16, 0.2 L/h at times 1, 2 and 3 h. We plot the substrate concentration S from the simulated process (blue line), from the Luenberger observer (red dash line) and from the algebraic equation (green line) in the same

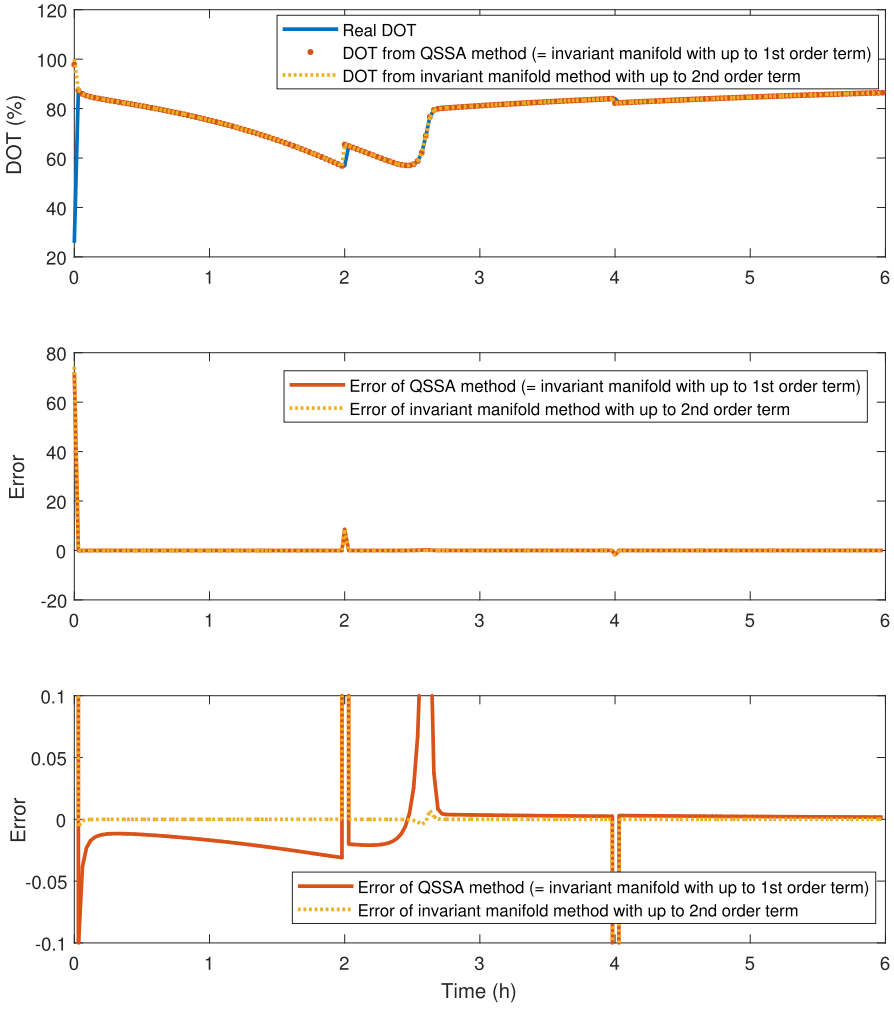

Fig. 5. Simulation of the fed-batch process under substrate limited condition.

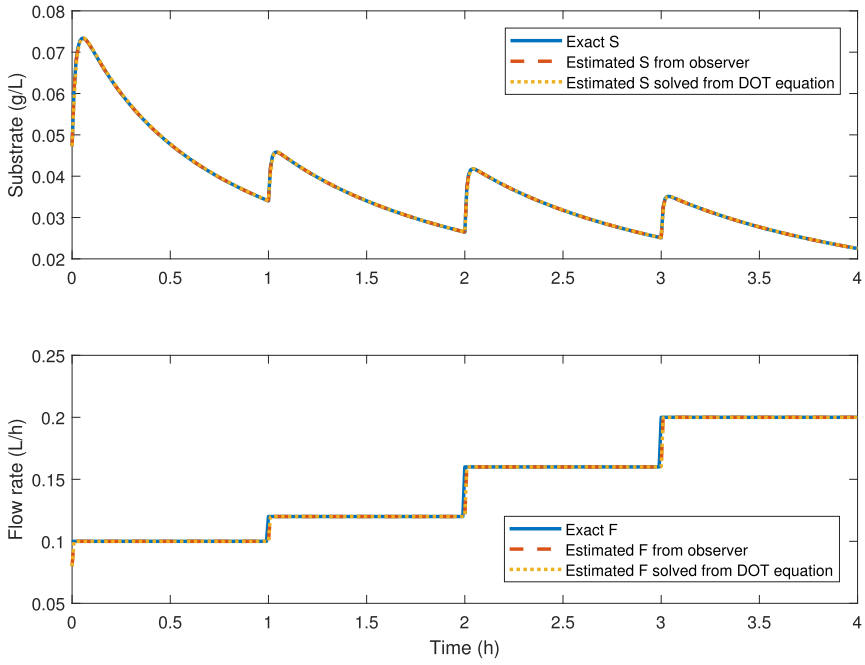

Fig. 6. State estimation with continuous measurement.

graph in Fig. 6. We can tell that both the observer and the solution from the function are in great agreement with the exact S and F during the entire time period, as they are nearly on top of each other.

Next, we consider the measurement of X to be discrete, sampled at every 0.2 h. There are several methods established to deal with discrete-time state estimation problems (Tatiraju et al., 1999; Ling and Kravaris, 2017; Ling et al., 2017a; Liu et al., 2015). To improve accuracy in the presence of large sampling periods, one could use a predictor w to estimate X between sampling points where there is no measurement (Ling et al., 2017b). At each sampling time point, w is reset to be the measurement of X. And between sampling points, it is simulated under the same dynamics of X. This method is demonstrated by the diagram of Fig. 7.

With the predictor, the full order observer becomes

$$\frac{d}{dt}\begin{bmatrix}\hat{S}\\ \hat{X}\\ D\hat{O}T\\ \hat{V}\\ \hat{F}\end{bmatrix}=\begin{bmatrix}-\frac{\hat{F}}{\hat{V}}\left(\hat{S}-S_{in}\right)-\hat{X}q_s\left(\hat{S},D\hat{O}T\right)\\ -\frac{\hat{F}}{\hat{V}}\hat{X}+Y_{x/s}\hat{X}q_s\left(\hat{S},D\hat{O}T\right)\\ K_La\left(DOT^*-D\hat{O}T\right)-HY_o\hat{X}q_s\left(\hat{S},D\hat{O}T\right)\\ \hat{F}\\ 0\end{bmatrix}+L\begin{bmatrix}w-\hat{X}\\ DOT-D\hat{O}T\\ V-\hat{V}\end{bmatrix}$$

$$\frac{dw}{dt}=-\frac{\hat{F}}{\hat{V}}w+Y_{x/s}wq_s\left(\hat{S},D\hat{O}T\right),t\in[t_k,t_{k+1})$$
$$w(t_{k+1})=X(t_{k+1}),t=t_{k+1}$$

For the reduced model, S would be solved from the algebraic Eq. (17) as $DOT=T(w,S,V)$, where w is the solution of

$$\begin{cases}\frac{dw}{dt}=-\frac{F}{V}w+Y_{x/s}wq_s(S_{solved},DOT),t\in[t_k,t_{k+1})\\ w(t_{k+1})=X(t_{k+1}),t=t_{k+1}\end{cases}$$

From Fig. 8, we observe that both methods show good performance in estimating the state S and parameter value F.

5. Discussion

In this work, we have studied model reduction problems for aerobic processes. For the very basic aerobic model, the analysis shows that the process typically consists of both fast and slow dynamics. Considering that the process is substrate-limited in practice, the slow and fast dynamics are connected in series and the dissolved oxygen tension is the fast state associated with the

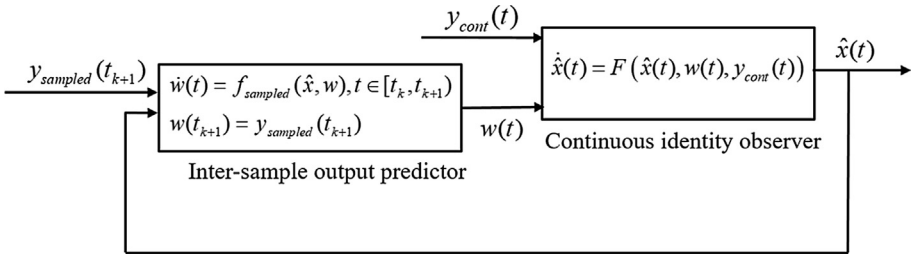

Fig. 7. Observer design scheme with inter sample predictor.

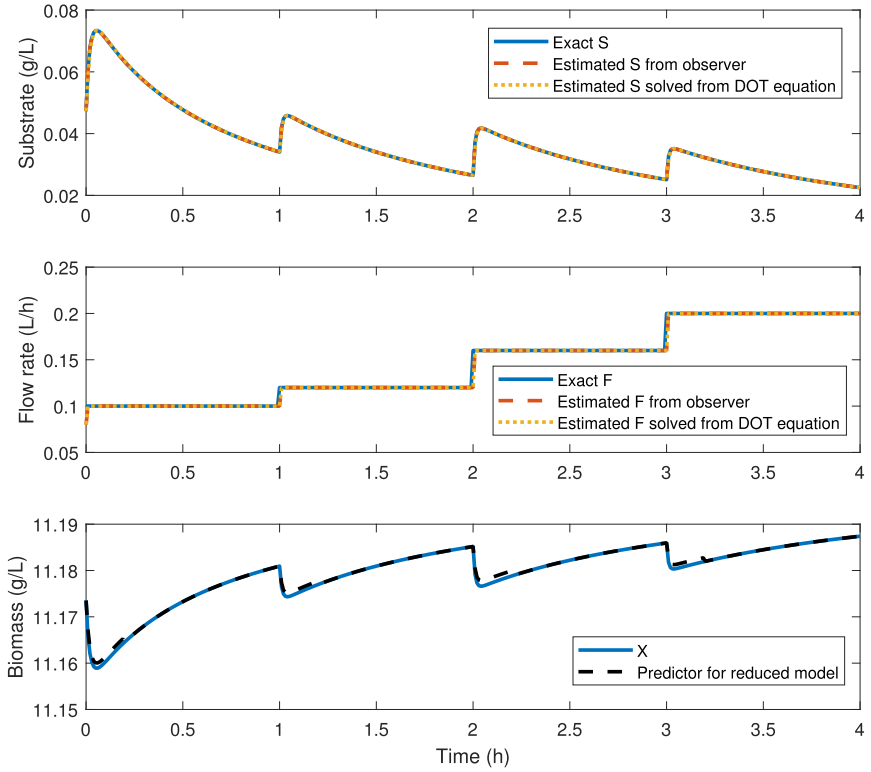

Fig. 8. State estimation with continuous DOT measurement and sampled X measurement.

fast eigenvalue. The numerical study on a macro-kinetic *E. coli* model also validates the aforementioned property. This is the theoretical basis that motivates the model reduction to eliminate the fast dynamics associated with the state *DOT*.

To reduce the model, we use the slow-motion invariant manifold to approximate the fast state *DOT*, by assuming the fast dynamics to be instantaneous. This is a rigorous model reduction method that guarantees the convergence to the real state once the fast dynamics dies out. To find the slow invariant manifold, a partial differential equation is approximately solved via perturbation analysis and the accuracy of the solution can be adjusted via the truncation order. As a comparison, the quasi steady state approximation, which is not accurate but easy to implement, is also used to find a reduced model. It turns out that the result of the QSSA method leads to the same first two terms in the asymptotic series for the slow-motion invariant manifold. It is observed that for typical aerobic processes, the less rigorous QSSA method leads to a model that is fairly accurate, while the slow-motion invariant manifold provides an even more precise approximation to the state *DOT*. The model reduction has been done to both continuous and fed-batch processes.

Finally, an observer design problem is studied as an example to show how this reduced model could be useful in bioengineering applications. With the reduced model, the traditional observer design problem can be simplified, leading to a zero-order observer, which becomes easy to use for lab researchers. The multi-rate measurement problem can also be handled with the introduction of an inter-sample predictor. And this zero-order observer shows great performance in estimating unmeasured states and unknown parameters.

6. Conclusion

Time scale analysis of certain dynamic systems reveals significant differences in the rate of change of their modes. This can be used as the basis to increase the tractability of differential equation models that describe processes governed by both fast and slow dynamics simultaneously. As we have demonstrated in this work, the stiffness of aerobic macro-kinetic models can be significantly reduced by the substitution of the differential equation for dissolved oxygen tension with an algebraic equation derived from the slow-motion invariant manifold. This significantly increases the tractability of the model in the sense of reducing the computational burden while increasing the robustness of the simulations, which will highly benefit those applications involving massive simulations (e.g. optimization and CFD simulations). Furthermore, the reduction of model may even open up possibilities for the use of some accessible PSE tools. For example, we show that the design of an observer based on the reduced model is simplified by assuming an instantaneous equilibrium between the dissolved oxygen and all other states. The simplification of the traditional observer to zero-order makes this powerful tool available for the scientific community of biotechnology, who has no need digging into the complicated aspects of mathematics but still can find a way to implement observers in order to improve their experiments. Although the derivation and proof is only performed for a basic aerobic model and an *E. coli* macro-kinetic growth model, this reduction approach can be used for any model with similar characteristics.

Declaration of Competing Interest

The authors declare that they have no known competing financial interests or personal relationships that could have appeared to influence the work reported in this paper.

Acknowledgments

Zhaoyang Duan and Costas Kravaris acknowledge financial support from the National Science Foundation through grant CBET-1706201.

References

Anane, E., López C, D.C., Neubauer, P., Cruz Bournazou, M.N., 2017. Modelling overflow metabolism in Escherichia coli by acetate cycling. Biochem. Eng. J. 125, 23–30.

Anane, E., García, Á.C., Haby, B., Hans, S., Krausch, N., Krewinkel, M., Hauptmann, P., Neubauer, P., Cruz Bournazou, M.N., 2019. Model-based framework for parallel scale down fed-batch cultivations in mini-bioreactors for accelerated phenotyping. Biotechnol. Bioeng.

Berlec, A., Štrukelj, B., 2013. Current state and recent advances in biopharmaceutical production in Escherichia coli, yeasts and mammalian cells. J. Industr. Microbiol. Biotechnol. 40 (3–4), 257–274.

Chiavazzo, E., Gorban, A.N., Karlin, I.V., 2007. Comparison of invariant manifolds for model reduction in chemical kinetics. Commun. Comput. Phys 2 (5), 964–992.

Cruz Bournazou, M.N., Arellano-Garcia, H., Wozny, G., Lyberatos, G., Kravaris, C., 2012. Asm3 extended for two-step nitrification–denitrification: a model reduction for sequencing batch reactors. J. Chem. Technol. Biotechnol. 87 (7), 887–896.

Dochain, D., 2003. State and parameter estimation in chemical and biochemical processes: a tutorial. J. Process Control 13 (8), 801–818.

Dochain, D., 2013. Automatic Control of Bioprocesses. John Wiley & Sons.

Duan, Z., Kravaris, C., 2018. Robust stabilization of a two-stage continuous anaerobic bioreactor system. AIChE J. 64 (4), 1295–1304.

Duan, Z., Cruz Bournazou, M.N., Kravaris, C., 2017. Dynamic model reduction for two-stage anaerobic digestion processes. Chem. Eng. J. 327, 1102–1116.

Duan, Z., Kravaris, C., 2017. Robust stabilization of a two-stage anaerobic bioreactor system. In: 2017 IEEE 56th Annual Conference on Decision and Control (CDC), IEEE, 2017, pp. 2083–2088.

Enfors, S.-O., Häggström, L., 2000. Bioprocess Technology: Fundamentals and Applications. Royal Institute of Technology.

Floudas, C.A., Gounaris, C.E., 2009. A review of recent advances in global optimization. J. Global Optim. 45 (1), 3–38.

Gavrilescu, M., Chisti, Y., 2005. Biotechnology–a sustainable alternative for chemical industry. Biotechnol. Adv. 23 (7–8), 471–499.

Gorban, A., 2018. Model reduction in chemical dynamics: slow invariant manifolds, singular perturbations, thermodynamic estimates, and analysis of reaction graph. Curr. Opin. Chem. Eng. 21, 48–59.

Gorban, A.N., Karlin, I.V., 2003. Method of invariant manifold for chemical kinetics. Chem. Eng. Sci. 58 (21), 4751–4768.

Gorban, A.N., Karlin, I.V., 2005. Invariant Manifolds for Physical and Chemical Kinetics, Vol. 660. Springer Science & Business Media.

Haby, B., Glauche, F., Hans, S., Cruz Bournazou, M.N., Neubauer, P., 2018. Stammcharakterisierung mittels on-line-redesign von experimenten. BIOspektrum 24 (1), 39–42.

Kalman, R.E., 1960. A New Approach to Linear Filtering And Prediction Problems. Journal of basic Engineering 82 (1), 35–45.

Kazantzis, N., Kravaris, C., 1998. Nonlinear observer design using lyapunov's auxiliary theorem. Syst. Control Lett. 34 (5), 241–247.

Kazantzis, N., Kravaris, C., Syrou, L., 2010. A new model reduction method for nonlinear dynamical systems. Nonlinear Dyn. 59 (1–2), 183.

Kokotovic, P.V., O'Malley Jr, R.E., Sannuti, P., 1976. Singular perturbations and order reduction in control theory–an overview. Automatica 12 (2), 123–132.

Koutinas, M., Kiparissides, A., Pistikopoulos, E.N., Mantalaris, A., 2012. Bioprocess systems engineering: transferring traditional process engineering principles to industrial biotechnology. Comput. Structural Biotechnol. J. 3 (4), e201210022.

Kravaris, C., Sotiropoulos, V., Georgiou, C., Kazantzis, N., Xiao, M., Krener, A.J., 2004. Nonlinear observer design for state and disturbance estimation. Proceedings of the 2004 American Control Conference, vol. 4. IEEE, pp. 2931–2936.

Krämer, D., King., R., 2019. A hybrid approach for bioprocess state estimation using NIR spectroscopy and a sigma-point Kalman filter. Journal of Process Control 82, 91–104.

Kravaris, C., Hahn, J., Chu, Y., 2013. Advances and selected recent developments in state and parameter estimation. Comput. Chem. Eng. 51, 111–123.

Kumar, A., Christofides, P.D., Daoutidis, P., 1998. Singular perturbation modeling of nonlinear processes with nonexplicit time-scale multiplicity. Chem. Eng. Sci. 53 (8), 1491–1504.

Ling, C., Kravaris, C., 2017. Multi-rate observer design for process monitoring using asynchronous inter-sample output predictions. AIChE J. 63 (8), 3384–3394.

Ling, C., Kravaris, C., 2017a. Multi-rate sampled-data observers based on a continuous-time design. In: 2017 IEEE 56th Annual Conference on Decision and Control (CDC), IEEE, 2017, pp. 3664–3669.

Ling, C., Kravaris, C., 2017b. Multi-rate sampled-data observers based on a continuous-time design. In: 2017 IEEE 56th Annual Conference on Decision and Control (CDC), IEEE, 2017, pp. 3664–3669.

Liu, A., Zhang, W.-A., Yu, L., Chen, J., 2015. Moving horizon estimation for multi-rate systems. In: 2015 54th IEEE Conference on Decision and Control (CDC), IEEE, 2015, pp. 6850–6855.

Luenberger, D.G., 1964. Observing the state of a linear system. IEEE Trans. Milit. Electron. 8 (2), 74–80.
Mears, L., Stocks, S.M., Albaek, M.O., Sin, G., Gernaey, K.V., 2017. Mechanistic fermentation models for process design. Monitor., Control, Trends Biotechnol. 35 (10), 914–924.
Möller, J., Kuchemüller, K.B., Steinmetz, T., Koopmann, K.S., Pörtner, R., 2019. Model-assisted design of experiments as a concept for knowledge-based bioprocess development. Bioprocess Biosyst. Eng., 1–16
Neubauer, P., Cruz Bournazou, M.N., Glauche, F., Junne, S., Knepper, A., Raven, M., 2013. Consistent development of bioprocesses from microliter cultures to the industrial scale. Eng. Life Sci. 13 (3), 224–238.
Okino, M.S., Mavrovouniotis, M.L., 1998. Simplification of mathematical models of chemical reaction systems. Chem. Rev. 98 (2), 391–408.
Psaltis, A., Kookos, I.K., Kravaris, C., 2013. Plant-wide control structure selection methodology based on economics. Comput. Chem. Eng. 52, 240–248.
Rabitz, H., Kramer, M., Dacol, D., 1983. Sensitivity analysis in chemical kinetics. Annu. Rev. Phys. Chem. 34 (1), 419–461.
Roussel, M.R., Fraser, S.J., 2001. Invariant manifold methods for metabolic model reduction. Chaos: An Interdiscip. J. Nonlinear Sci. 11 (1), 196–206.
Segel, L.A., Slemrod, M., 1989. The quasi-steady-state assumption: a case study in perturbation. SIAM Rev. 31 (3), 446–477.
Stamatelatou, K., Syrou, L., Kravaris, C., Lyberatos, G., 2009. An invariant manifold approach for cstr model reduction in the presence of multi-step biochemical reaction schemes. application to anaerobic digestion. Chem. Eng. J. 150 (2–3), 462–475.
Tatiraju, S., Soroush, M., Ogunnaike, B.A., 1999. Multirate nonlinear state estimation with application to a polymerization reactor. AIChE J. 45 (4), 769–780.
Wang, R., Koppram, R., Olsson, L., Franzén, C.J., 2014. Kinetic modeling of multi-feed simultaneous saccharification and co-fermentation of pretreated birch to ethanol. Bioresour. Technol. 172, 303–311.
Wang, R., Unrean, P., Franzén, C.J., 2016. Model-based optimization and scale-up of multi-feed simultaneous saccharification and co-fermentation of steam pre-treated lignocellulose enables high gravity ethanol production. Biotechnol. Biofuels 9 (1), 88.
Welch, G., Bishop, G., et al., An introduction to the kalman filter.
Westman, J.O., Franzén, C.J., 2015. Current progress in high cell density yeast bioprocesses for bioethanol production. Biotechnol. J. 10 (8), 1185–1195.